

## Interplay Between pVHL and mTORC1 Pathways in Clear-Cell Renal Cell Carcinoma

Blanka Kucejova<sup>1,2,6</sup>, Samuel Peña-Llopis<sup>1,2,6</sup>, Toshinari Yamasaki<sup>1,2,6</sup>, Sharanya Sivanand<sup>1,2,6</sup>, Tram Anh T. Tran<sup>1,2,6</sup>, Shane Alexander<sup>1,2,6</sup>, Nicholas C. Wolff<sup>1,2,6</sup>, Yair Lotan<sup>3</sup>, Xian-Jin Xie<sup>4,6</sup>, Wareef Kabbani<sup>5</sup>, Payal Kapur<sup>5</sup>, and James Brugarolas<sup>1,2,6</sup>

### Abstract

mTOR complex 1 (mTORC1) is implicated in cell growth control and is extensively regulated. We previously reported that in response to hypoxia, mTORC1 is inhibited by the protein regulated in development and DNA damage response 1 (REDD1). *REDD1* is upregulated by hypoxia-inducible factor (HIF)-1, and forced *REDD1* expression is sufficient to inhibit mTORC1. REDD1-induced mTORC1 inhibition is dependent on a protein complex formed by the tuberous sclerosis complex (TSC)1 and 2 (TSC2) proteins. In clear-cell renal cell carcinoma (ccRCC), the von Hippel-Lindau (*VHL*) gene is frequently inactivated leading to constitutive activation of HIF-2 and/or HIF-1, which may be expected to upregulate REDD1 and inhibit mTORC1. However, mTORC1 is frequently activated in ccRCC, and mTORC1 inhibitors are effective against this tumor type; a paradox herein examined. *REDD1* was upregulated in *VHL*-deficient ccRCC by *in silico* microarray analyses, as well as by quantitative real-time PCR, Western blot, and immunohistochemistry. *Vhl* disruption in a mouse model was sufficient to induce *Redd1*. Using ccRCC-derived cell lines, we show that REDD1 upregulation in tumors is *VHL* dependent and that both HIF-1 and HIF-2 are, in a cell-type-dependent manner, recruited to, and essential for, *REDD1* induction. Interestingly, whereas mTORC1 is responsive to REDD1 in some tumors, strategies have evolved in others, such as mutations disrupting *TSC1*, to subvert mTORC1 inhibition by REDD1. Sequencing analyses of 77 ccRCCs for mutations in *TSC1*, *TSC2*, and *REDD1*, using *PTEN* as a reference, implicate the *TSC1* gene, and possibly *REDD1*, as tumor suppressors in sporadic ccRCC. Understanding how ccRCCs become refractory to REDD1-induced mTORC1 inhibition should shed light into the development of ccRCC and may aid in patient selection for molecular-targeted therapies. *Mol Cancer Res*; 9(9): 1255–65. ©2011 AACR.

### Introduction

mTOR complex 1 (mTORC1) is implicated in the pathogenesis of renal cell carcinoma (RCC), including clear-cell type (ccRCC). mTORC1 is thought to be activated in 60% to 85% of ccRCCs (1, 2), and mTORC1 inhibitors have been shown in 2 phase III clinical trials to delay tumor progression (3, 4). However, how mTORC1 is deregulated in ccRCCs is poorly understood.

mTOR is an atypical serine/threonine protein kinase. mTOR nucleates 2 different complexes, mTORC1 and mTORC2, which modify different substrates (5). mTORC1 is composed of mTOR and an adaptor protein, regulatory associated protein of mTOR (raptor; ref. 6). Other proteins are found in mTORC1, including mammalian lethal with sec-thirteen protein 8, which at least during development, is dispensable for mTORC1 function (6). mTORC1 is involved in regulating cell growth, and the two best studied substrates of mTORC1 are S6 kinase 1 (S6K1) and the eukaryotic initiation factor 4E (eIF4E)-binding protein 1 (4E-BP1; ref. 7). By phosphorylating S6K1 and 4E-BP1, mTORC1 stimulates protein translation. Importantly, only mTORC1 is directly inhibited by rapamycin (also called sirolimus; ref. 5).

mTORC1 activity is tightly controlled. Regulation of mTORC1 in response to hypoxia involves the protein regulated in development and DNA damage response 1 (REDD1, also called DNA-damage-inducible transcript 4; ref. 8). REDD1 is an evolutionarily conserved protein with a novel fold (9) that is upregulated in response to hypoxia in most cell types (8, 10–14). Hypoxia leads to the stabilization of the  $\alpha$  subunits of the heterodimeric ( $\alpha/\beta$ ) hypoxia-inducible factor (HIF)-1 and -2 transcription factors and increased expression

**Authors' Affiliations:** Departments of <sup>1</sup>Developmental Biology, <sup>2</sup>Internal Medicine, Oncology Division, <sup>3</sup>Urology, <sup>4</sup>Clinical Sciences, <sup>5</sup>Pathology, and <sup>6</sup>Simmons Comprehensive Cancer Center, University of Texas Southwestern Medical Center, Dallas, Texas

**Note:** Supplementary data for this article are available at Molecular Cancer Research Online (<http://mcr.aacrjournals.org/>).

B. Kucejova and S. Peña-Llopis contributed equally to this work.

**Corresponding Author:** James Brugarolas, Department of Internal Medicine, University of Texas Southwestern Medical Center, Dallas, TX, 75390. Phone: 214-648-4059; Fax: 214-648-1960; E-mail: James.Brugarolas@UTSouthwestern.edu

doi: 10.1158/1541-7786.MCR-11-0302

©2011 American Association for Cancer Research.

of their target genes. HIF-1 has been shown to bind to a response element in the *REDD1* promoter and is required, at least in some cell types, for *REDD1* induction (10). *REDD1* negatively regulates mTORC1 and simply overexpressing *REDD1* is sufficient to inhibit mTORC1 (8).

*REDD1*-induced mTORC1 inhibition requires the complex formed by the tuberous sclerosis complex 1 and 2 (TSC1/TSC2) proteins (8). TSC2 acts as GTPase-activating protein toward a small G protein, Ras homologue enriched in brain (Rheb), which plays an important role in mTORC1 activation (15). Disruption of TSC1/TSC2 blocks mTORC1 inhibition by *REDD1* (8, 16, 17). How *REDD1* functions remains to be elucidated. Previously, the TSC2 protein was found to bind 14-3-3 proteins (18), and *REDD1* has been proposed to act by directly binding to and sequestering 14-3-3 proteins away from TSC2 (19). However, critical residues in the putative 14-3-3 binding motif in *REDD1* are not conserved (9). In addition, the presumed motif does not conform to any 14-3-3 binding motif known and cannot be docked onto 14-3-3 $\beta$  without steric clashes (9).

The TSC1/TSC2 complex is inactivated in the eponymous syndrome, TSC, which is characterized by hamartomas in multiple organs (20). Although TSC patients exhibit an increased predisposition to develop RCC, which tends to occur at an earlier age than in the general population (20), mutations in *TSC1* or *TSC2* have not been found in sporadic ccRCC (21).

ccRCCs are characteristically associated with disruption of the tumor suppressor gene von Hippel-Lindau (*VHL*), which is located in 3p25-26, and which, in recent studies, has been found inactivated in up to 90% of sporadic tumors (22). The *VHL* gene encodes a protein (pVHL) that functions as the substrate recognition subunit of an E3 ubiquitin ligase complex that targets, among others, the  $\alpha$  subunits of HIF-1 and HIF-2 for degradation (23). *VHL* disruption results in constitutive activation of HIF-2 (and/or HIF-1) in tumors and increased expression of their target genes (24).

Because *REDD1* is an HIF-1 target gene (10), *REDD1* may be upregulated in *VHL*-deficient ccRCCs where it would be expected to downregulate mTORC1. Paradoxically, mTORC1 seems to be broadly activated in ccRCC (1, 2), and mTORC1 inhibitors are effective against this disease (3, 4). Herein, this paradox was examined.

## Materials and Methods

### Tissue processing

Tumor and normal renal cortex samples were collected from surgical specimens following informed consent of an Institutional Review Board approved tissue collection protocol and were flash frozen in liquid nitrogen and stored at  $-80^{\circ}\text{C}$ . From each sample, immediately flanking sections from 2 sides perpendicular to each other were processed for hematoxylin and eosin (H&E) staining and analyzed by a pathologist (W.K.) for composition (tumor content) and quality (hemorrhage and necrosis). Tissues were selected and processed according to Peña-Llopis and colleagues (unpublished data).

### *VHL* reconstitution

786-O, A498, and Caki-2 cells were transfected using TransIT-LT1 Transfection Reagent (Mirus) with pcDNA3.1/Hygro/HA-VHL (laboratory database ID #586) or empty vector (pcDNA3.1/Hygro; ID #338), and polyclonal populations were selected and maintained in Hygromycin (250  $\mu\text{g}/\text{mL}$ ).

### siRNA transfections

siRNA oligonucleotides were from Dharmacon and Dicer-substrate siRNAs (DsiRNA) duplexes from Integrated DNA Technologies. Transfections were carried out using Lipofectamine 2000 (Invitrogen) for A498 or DharmaFECT reagent 3 (Dharmacon) for 786-O and Caki-2 cells according to manufacturer instructions using 220 pmol of siRNA and 20 pmol of DsiRNA per well of a 6-well plate. Sequences or catalogue numbers are listed in Supplementary Table S2.

### Sequencing of *TSC1*, *TSC2*, *REDD1*, and *PTEN*

Bidirectional DNA sequencing was carried out following PCR amplification using primers designed to produce 400 to 600 bp amplicons and to include at least 50 bp from intron/exon boundaries. Unless otherwise indicated, only bidirectionally observed somatic mutations are reported.

### Statistics

All data are presented as means with SDs unless otherwise specified. *P* values are calculated by 2-tailed Student's *t* test assuming equal variances unless otherwise indicated. Correlations were calculated using Spearman's  $\rho$  in SPSS Statistics 17.0.

For additional information, see Supplementary material.

## Results

### *REDD1* regulation by pVHL

Recently, we reported that intravenous administration of adenovirus-Cre (Ad-Cre) to *Vhl*<sup>F/F</sup> mice (also referred to as *Vhl*<sup>flloxP/flloxP</sup>) led to *Vhl* inactivation and constitutive Hif activation in hepatocytes phenocopying the lipid accumulation observed in ccRCC (25). Using this system, we examined whether *Vhl* loss was sufficient to induce *Redd1*. *Vhl* disruption (Fig. 1A) led to Hif activation (as determined by the upregulation of the Hif target gene *Glut1*; Fig. 1B) and *Redd1* induction, which was observed at the mRNA (Fig. 1B) and protein levels (Fig. 1C). Thus, *Vhl* loss is sufficient to induce *Redd1* expression.

To examine *REDD1* regulation by pVHL in ccRCC, we selected a panel of ccRCC-derived cell lines (786-O, A498, and Caki-2). These cell lines have undergone loss of heterozygosity (LOH) at the *VHL* locus and contain a single mutant *VHL* allele (26). However, whereas pVHL function is completely disrupted in 786-O and A498 cells, which harbor truncating mutations upstream of the  $\alpha$ -domain, which contains the elongin C binding motif, the  $\alpha$ -domain is only partially truncated in Caki-2 cells

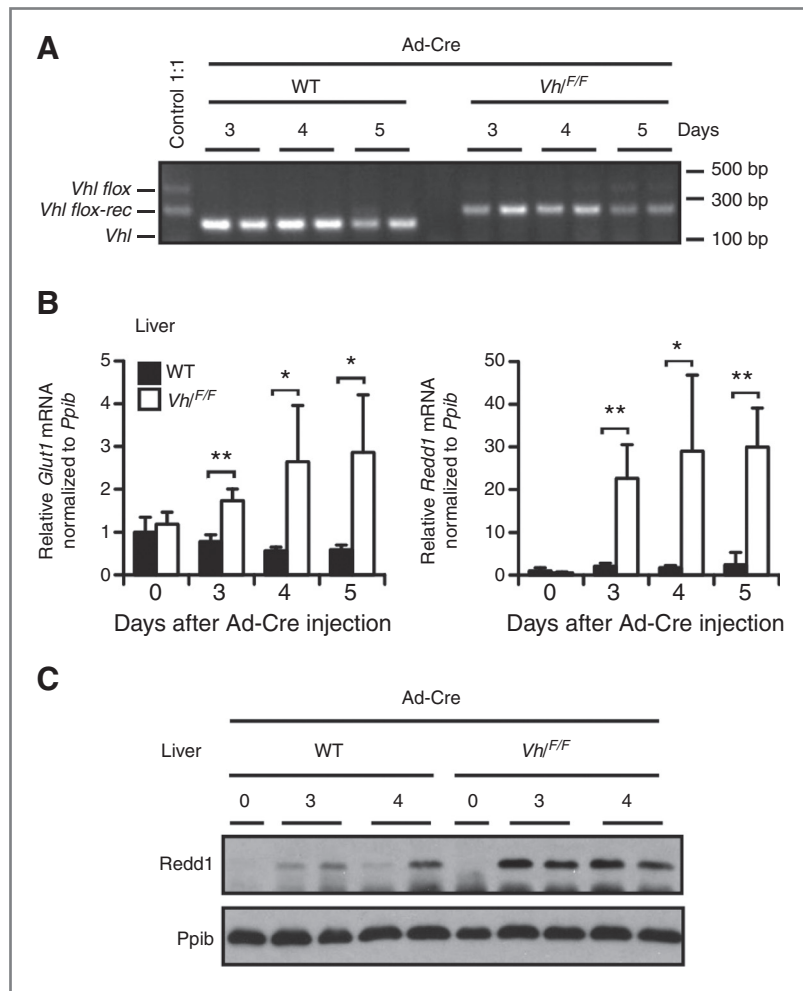


**Figure 1.** Acute *Vhl* disruption in mouse hepatocytes, which phenocopies important aspects of *VHL* loss in renal carcinoma cells in humans, is sufficient to upregulate *Redd1*. A, PCR of genomic DNA extracted from wild-type (WT) and *Vhl*<sup>F/F</sup> livers after the indicated number of days following intravenous administration of Ad-Cre; as a control, a 1:1 mixture of DNA containing fully recombined *Vhl*<sup>F</sup> (*Vhl flox-rec*) and unrecombined (*Vhl flox*) alleles is shown. B, qRT-PCR of livers from WT and *Vhl*<sup>F/F</sup> animals injected with Ad-Cre. Data are normalized to cyclophilin (*Ppib*) and represent averages with SD ( $n = 3-6$ ); \*,  $P < 0.05$ ; \*\*,  $P < 0.01$  (unpaired *t* test). C, immunoblot of extracts from livers from WT and *Vhl*<sup>F/F</sup> animals injected with Ad-Cre.

(26). Nevertheless, the *VHL* mutation in Caki-2 cells (c.529A > T, Supplementary Fig. S1) is likely to be pathogenic as other somatic mutations in ccRCC have been identified downstream (both missense as well as truncating; ref. 27). Another difference among the cell lines is that in 786-O and A498 HIF-2 $\alpha$  is upregulated and HIF-1 $\alpha$  is undetectable, whereas in Caki-2 cells, the reciprocal pattern is observed.

To determine whether REDD1 was upregulated in ccRCC as a consequence of *VHL* loss, we examined the effects of stable reconstitution with wild-type *VHL*. Ectopic *VHL* was expressed at different levels across the cell lines (Fig. 2A and data not shown), and as expected, the levels were lower than in previously selected monoclonal populations of reconstituted 786-O cells (28). Nevertheless, *VHL* reconstitution uniformly downregulated the levels of HIF- $\alpha$  and its target Glut-1 (Fig. 2A–D, Supplementary Fig. S2). In addition, *VHL* expression similarly downregulated REDD1 (Fig. 2A–D, Supplementary Fig. S2). Furthermore, *VHL* reconstitution restored the normal regulation of HIF- $\alpha$  and REDD1 by hypoxia (Fig. 2A–D, Supplementary Fig. S2). In keeping with the idea that endogenous mutant *VHL* in Caki-2 cells retains some functionality,

baseline REDD1 levels were lower in these cells (Fig. 2A). Furthermore, the effects of *VHL* reconstitution on REDD1 induction by hypoxia in Caki-2 cells were incremental (Fig. 2D). Taken together these data show that REDD1 is induced in ccRCC cell lines as a consequence of *VHL* disruption and that REDD1 levels and its normal regulation can be restored by *VHL* reconstitution.

#### HIF- $\alpha$ -dependent regulation of REDD1 in ccRCC

To unequivocally determine whether REDD1 regulation by pVHL involved HIF and whether both HIF-1 and HIF-2 were implicated, we carried out both chromatin immunoprecipitation (ChIP) as well as knockdown experiments. ChIP was conducted using antibodies against the aryl hydrocarbon receptor nuclear translocator (ARNT, also called HIF-1 $\beta$ ) as well as the corresponding HIF- $\alpha$  subunit [HIF-2 $\alpha$  (786-O and A498) and HIF-1 $\alpha$  (Caki-2)]. *VHL*-reconstituted cell lines were used as a control. As a reference, the amount of HIF bound to the HIF target genes phosphoglycerate kinase (*PGK1*) and lactate dehydrogenase A (*LDHA*) was measured.

As expected, ARNT and HIF- $\alpha$  were observed bound to *PGK1* and *LDHA* sequences, and the amount decreased

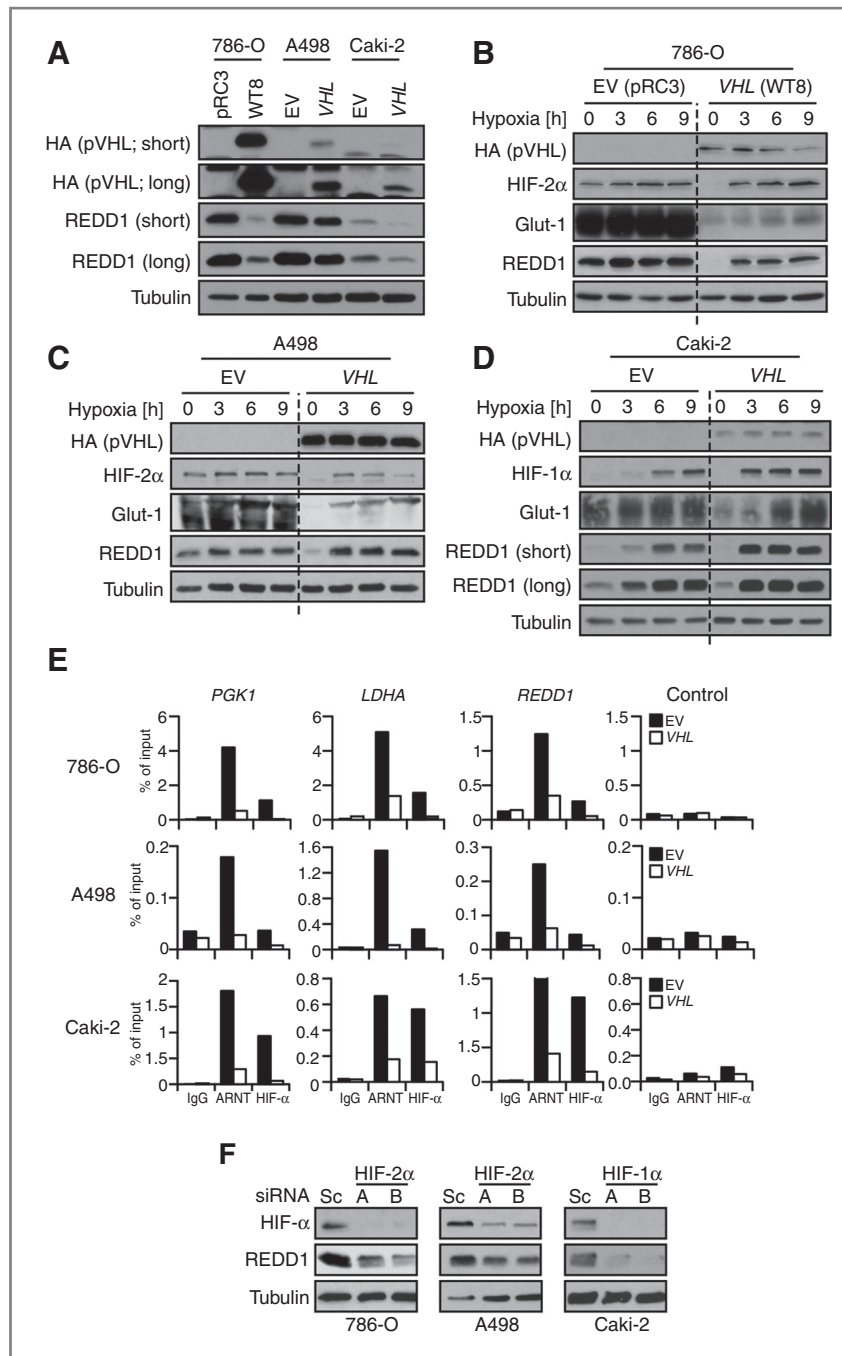


**Figure 2.** HIF- and pVHL-dependent regulation of REDD1 in ccRCC. A–D, immunoblot of protein extracts (heat-denatured or not [Glut-1]) from ccRCC cell lines reconstituted with HA-VHL (VHL) or an empty vector (EV), compared with monoclonal populations of 786-O cells reconstituted with HA-VHL (WT8) or an EV (pRC3), and exposed to hypoxia (where indicated) for the stated number of hours. E, ChIP using antibodies for ARNT and HIF- $\alpha$  (HIF-2 $\alpha$  for both 786-O and A498; and HIF-1 $\alpha$  for Caki-2) versus rabbit IgG control in VHL or EV stably transfected cell lines evaluated for the indicated genes or a region far upstream of VEGF used as a control. F, immunoblot of ccRCC cell lines transfected with 2 independent siRNAs targeting HIF-2 $\alpha$  (786-O, A498) or HIF-1 $\alpha$  (Caki-2) versus scrambled (Sc) control.

following VHL reconstitution (Fig. 2E, see also an independent experiment in Supplementary Fig. S3). Similarly, increased levels of ARNT and HIF- $\alpha$  were detected on REDD1 (Fig. 2E, Supplementary Fig. S3).

To determine whether HIF was required for REDD1 upregulation, the effects of depleting HIF- $\alpha$  subunits were evaluated using 2 independent siRNAs. Knockdown of either HIF-2 $\alpha$  (in 786-O and A498) or HIF-1 $\alpha$  (in Caki-2) downregulated REDD1 levels (Fig. 2F). Taken together these data show that VHL disruption results in an

HIF-dependent direct upregulation of REDD1. Furthermore, unlike some genes that seem to be selectively regulated by HIF-1 or HIF-2 (29, 30), our results show that both HIF-1 and HIF-2 can mediate the upregulation of REDD1 in ccRCC.

#### REDD1 is highly expressed in VHL-deficient ccRCC tumors

Next, we evaluated whether REDD1 expression was upregulated in ccRCC tumors. For these experiments,

we analyzed 2 previously reported, publicly available, microarray data sets (31, 32). We selected tumors with mutant *VHL* and evaluated *REDD1* expression levels by comparison with normal kidney samples. The pattern of *REDD1* expression was correlated to that of a cohort of hypoxia-inducible genes, largely HIF-1 and HIF-2 targets (30, 33–35), found to be upregulated in ccRCC. In addition, as a reference, a second gene cohort was selected of genes implicated in ccRCC pathogenesis that for the most part are not regulated by HIF or upregulated in ccRCC (Fig. 3A). This analysis showed

that *REDD1* was upregulated in *VHL*-mutant ccRCCs ( $Q = 6 \times 10^{-12}$ ) and that *REDD1* upregulation was indistinguishable from that of other HIF target genes (Fig. 3A).

In an independent tumor cohort, we compared tumors harboring *VHL* mutations or *VHL* gene methylation with normal renal cortices (from where ccRCC is thought to arise) as well as with ccRCCs with presumed intact *VHL* function. This analysis showed that *REDD1* was upregulated in *VHL*-deficient ccRCCs, by comparison with normal cortices, and that substantially more heterogeneity

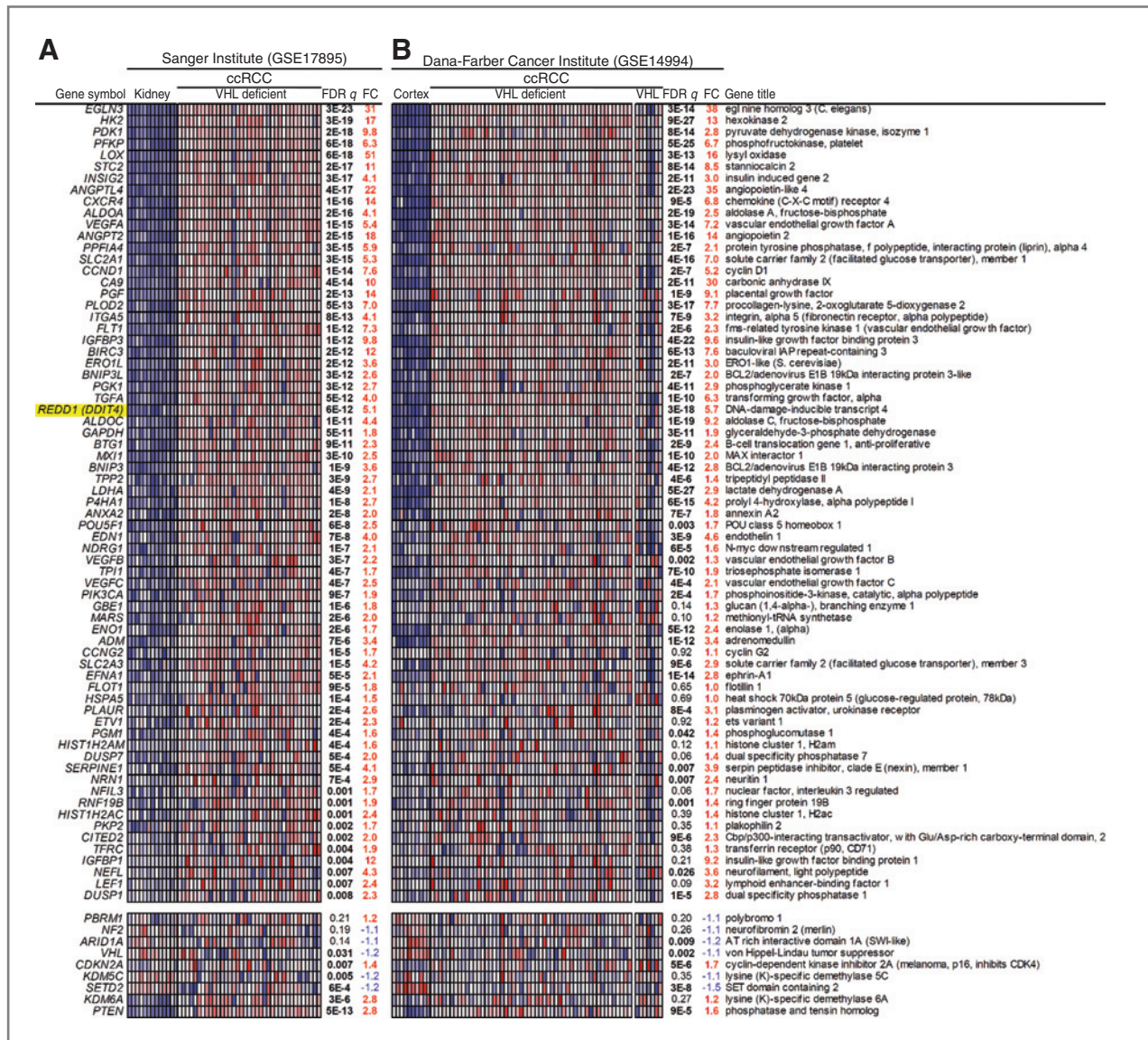


**Figure 3.** *REDD1* is upregulated in *VHL*-deficient ccRCCs. A, heatmap representation of *REDD1* expression levels compared with other hypoxia-inducible genes and a panel of other genes (bottom) in ccRCCs with *VHL* mutations compared with normal kidney samples from GSE17895; genes are ranked by FDR *q* of ccRCC versus kidney expression values. B, heatmap representation of gene expression values for the same genes as in A from GSE14994 in tumors with *VHL* mutations or *VHL* gene methylation (*VHL* deficient) versus normal renal cortices or a set of tumors with no evidence of *VHL* mutation or methylation. In both A and B, bold FDR *Q* values are statistically significant; in red and blue are the fold change (FC) values for genes that are upregulated or downregulated, respectively.

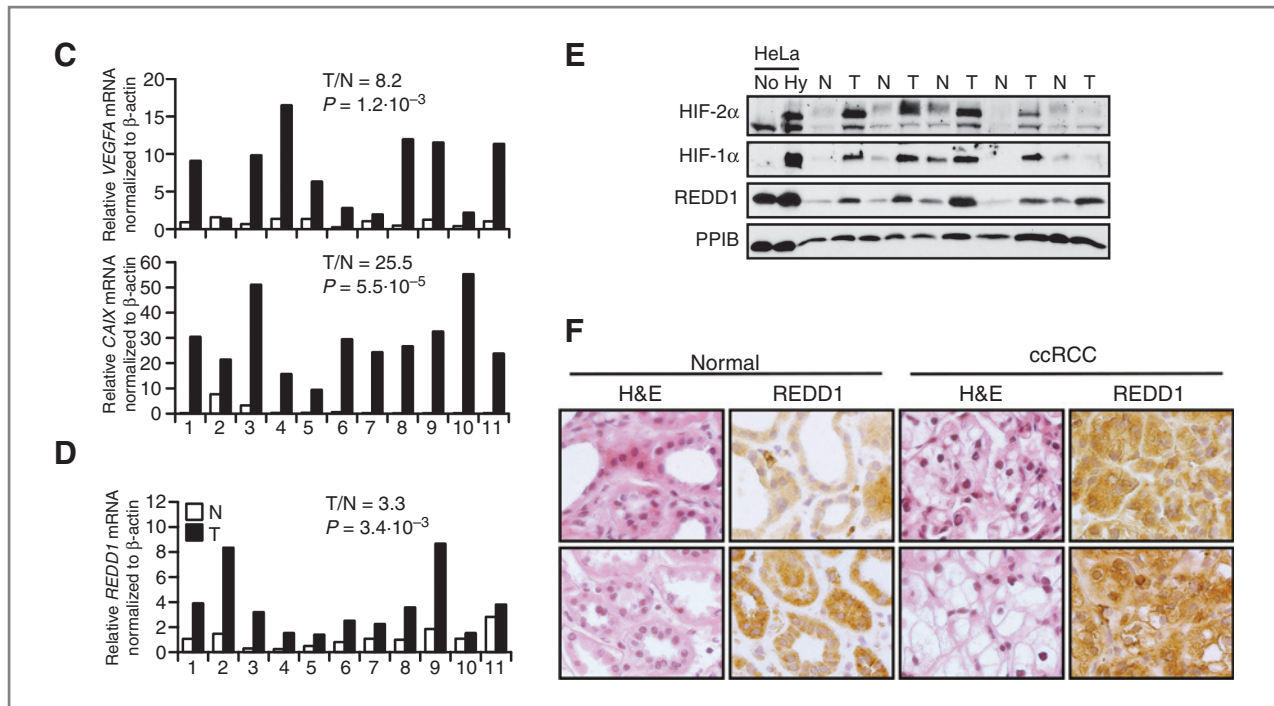


**Figure 3.** (Continued) C, qRT-PCR of *VEGFA*, *CAIX* as well as *REDD1* (D) expression levels in tumors (T) and paired normal (N) renal cortical samples from the same patients. Ratios of tumor to normal (T/N) and *P* values (calculated by paired *t* tests) are shown. E, immunoblot of paired normal (N) and tumor (T) samples; HeLa cells in normoxia (No) or hypoxia (Hy) shown as controls; cyclophilin B (PPIB) was used as a loading indicator. F, immunohistochemistry analysis of REDD1 in representative normal kidney and ccRCC samples.

existed in *REDD1* levels in ccRCCs with presumed wild-type *VHL* (Fig. 3B).

To further establish that *REDD1* was upregulated in *VHL*-deficient ccRCC, we evaluated the expression of *REDD1* in a cohort of fresh-frozen ccRCC tumors containing *VHL* mutations and compared the levels with matched normal renal cortices from the same patients. As a reference, quantitative real-time PCR (qRT-PCR) was carried out for several HIF targets. By comparison with the corresponding normal cortices, *CAIX* and *VEGFA* expression was upregulated in tumors ( $P = 5.5 \times 10^{-5}$  and  $1.2 \times 10^{-3}$ , respectively, paired *t* test, Fig. 3C). Similarly, *REDD1* was upregulated in *VHL*-deficient ccRCCs with an overall increase in expression of approximately 3.3-fold ( $P = 3.4 \times 10^{-3}$ , paired *t* test, Fig. 3D).

We evaluated REDD1 protein levels in tumor lysates and tissue sections using a monoclonal anti-REDD1 antibody we generated. This antibody recognized REDD1 both by Western blot and immunoprecipitation and appeared to be highly specific (Supplementary Fig. S4). REDD1 protein levels were consistently upregulated in *VHL*-deficient ccRCCs (Fig. 3E). In normal kidneys, REDD1 was found to be expressed in normal renal tubular cells (Fig. 3F), and these results were consistent with observations in hypoxic mice (36). Overall, the pattern of staining appeared to be diffusely cytoplasmic (Fig. 3F). In tumors, REDD1 levels were substantially elevated (Fig. 3F). Next, we examined REDD1 levels by

IHC in an unselected cohort of 78 ccRCCs. REDD1 was highly expressed in the vast majority of tumors (Supplementary Table S1).

We previously reported that REDD1 is a critical negative regulator of mTORC1 and that *REDD1* overexpression was sufficient to inhibit mTORC1 (8). However, mTORC1 has been reported to be active in 60% to 85% of ccRCCs (1, 2). We examined the same tumor cohort for mTORC1 activation. As a readout, we evaluated the phosphorylation of S6 at S235/236 and S240/244. A statistically significant correlation was found between phospho-S6<sup>S240/244</sup>, which is thought to be more specific for mTORC1 (37) and phospho-S6<sup>S235/236</sup> ( $P < 0.001$ ), and some level of S6<sup>S240/244</sup> phosphorylation was observed in 80% of tumors (Supplementary Table S1). Not unexpectedly, given that the majority of tumors stained positively for phospho-S6 and REDD1, there was a significant overlap (Supplementary Table S1).

#### mTORC1 regulation by REDD1 in ccRCC

To begin to explore this paradox, we asked whether REDD1 was involved in regulating mTORC1 in ccRCC. Should REDD1 be regulating mTORC1 in ccRCC cell lines, REDD1 knockdown should increase mTORC1 activity. For these experiments, cell lines were grown in 1% serum, which more likely mimics the growth factor milieu of tumors. In both A498 and Caki-2 cells, REDD1 knockdown increased S6 phosphorylation (Fig. 4A) and reduced

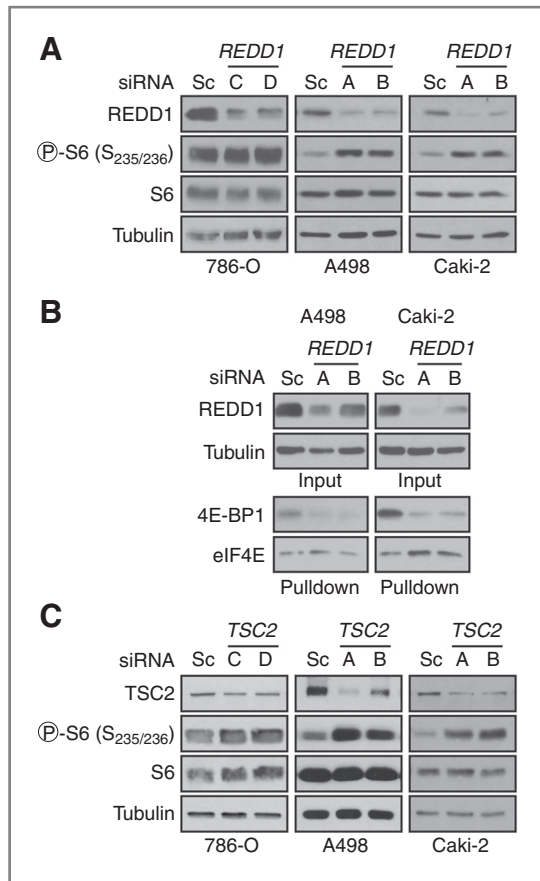


**Figure 4.** Cell type-dependent regulation of mTORC1 by REDD1 and the TSC1/TSC2 complex. A, Western blot and (B) m<sup>7</sup>GTP affinity chromatography of the indicated cell lines treated with siRNAs targeting REDD1 versus a scrambled control (Sc). C, Western blot of cells grown as in (A) but treated with siRNA against TSC2.

4E-BP1 binding to eIF4E (Fig. 4B). Thus, REDD1 normally inhibits mTORC1 in these cells. By contrast, REDD1 knockdown had practically no effect on mTORC1 readouts in 786-O cells (Fig. 4A and data not shown).

Because the TSC1/TSC2 complex is required for mTORC1 regulation by REDD1 (8, 16, 17), we examined the effects of TSC2 depletion. Similar to the effects of REDD1 knockdown, S6 phosphorylation was upregulated in TSC2-depleted A498 and Caki-2 cells but not in 786-O cells (Fig. 4C). These data show that in both A498 and Caki-2 cells, mTORC1 activity is restrained by REDD1 and the TSC1/TSC2 complex. By contrast, mTORC1 activity seems to be uncoupled from both REDD1 and TSC1/TSC2 in 786-O cells, which are *PTEN* deficient (38). No mutations are observed in *TSC1* or *TSC2* in 786-O cells (38), and we speculate that TSC1/TSC2 may be inactivated posttranslationally as a result of increased Akt activity due to *PTEN* loss. As the TSC1/TSC2 complex is required for REDD1-induced mTORC1 inhibition (8, 16, 17), these results would provide an explanation for mTORC1 activation in these cells despite high REDD1 levels. Furthermore,

the finding that in 786-O cells mTORC1 was uncoupled from REDD1 provided an explanation for the coexistence of high REDD1 levels with mTORC1 activation in ccRCC. However, *PTEN* mutations are rare in ccRCC (39–41), and we sought to explore this further.

### ***TSC1* is a tumor suppressor in sporadic ccRCC**

We set out to examine other components of the mTORC1 pathway. A previous study failed to identify mutations in *TSC1* or *TSC2* in ccRCC (21). However, the study involved a small number of tumors, and we were encouraged by the finding during a whole-genome sequencing study (Peña-Llopis and colleagues, unpublished data) of a somatically acquired mutation in *TSC1*, which we sought to characterize. The mutation, which was accompanied by LOH, was a splice site mutation in the exon 5 splice acceptor (IVS211-2A > T; Fig. 5A). This mutation, as determined by RT-PCR and cDNA sequencing, led to exon 5 skipping (Fig. 5B and C). Exon 5 loss, however, would be predicted not alter the reading frame. To assess the results of exon 5 skipping, a *TSC1*<sup>ΔEx5</sup> cDNA was generated by site-directed mutagenesis and was introduced into immortalized *Tsc1*-deficient mouse embryo fibroblasts (MEF). In contrast to *Tsc1*<sup>-/-</sup> MEFs reconstituted with wild-type human *TSC1*, *TSC1*<sup>ΔEx5</sup>-reconstituted MEFs expressed very low protein levels (Fig. 5D). This was not because of low *TSC1*<sup>ΔEx5</sup> mRNA expression (Fig. 5E and F), and experiments with a proteasome inhibitor suggested that the *TSC1*<sup>ΔEx5</sup> protein was unstable (Fig. 5G). Because TSC1 functions to stabilize TSC2, not surprisingly, TSC2 protein levels were substantially reduced in *TSC1*<sup>ΔEx5</sup>-reconstituted MEFs (Figs 5D and G).

Next, we tested the functional consequences of *TSC1*<sup>ΔEx5</sup> expression on mTORC1. Serum starvation, which downregulated mTORC1 activity in wild-type *TSC1* expressing cells, failed to downregulate mTORC1 in *TSC1*<sup>ΔEx5</sup>-reconstituted cells (Fig. 5H). Finally, to determine whether *TSC1*<sup>ΔEx5</sup> would uncouple mTORC1 from REDD1, we evaluated the response of *TSC1*<sup>ΔEx5</sup>-expressing cells to hypoxia, which results in a *Redd1*-dependent inhibition of mTORC1 (8). As shown in Figure 5I, despite substantial upregulation of *Redd1* in response to hypoxia, *TSC1*<sup>ΔEx5</sup>-reconstituted cells, like empty vector reconstituted cells, failed to inhibit mTORC1. Taken together these data show that *TSC1* (IVS211-2A > T) results in exon 5 loss and an unstable protein leading to constitutive mTORC1 activation and its uncoupling from REDD1.

Having established a precedent for an inactivating somatically acquired *TSC1* mutation in ccRCC, and while suspecting based on the previous study (21) that the *TSC1* mutation frequency in ccRCC may be low, we set out to determine whether additional *TSC1* mutations could be found in ccRCC. For these experiments, we carried out PCR amplification and bidirectional capillary sequencing analyses of *TSC1* coding sequences (and splice sites) in the aforementioned cohort of 77 fresh-frozen ccRCCs specimens, including 71 tumors for which we had matched normal samples. Interestingly, 3 additional mutations in

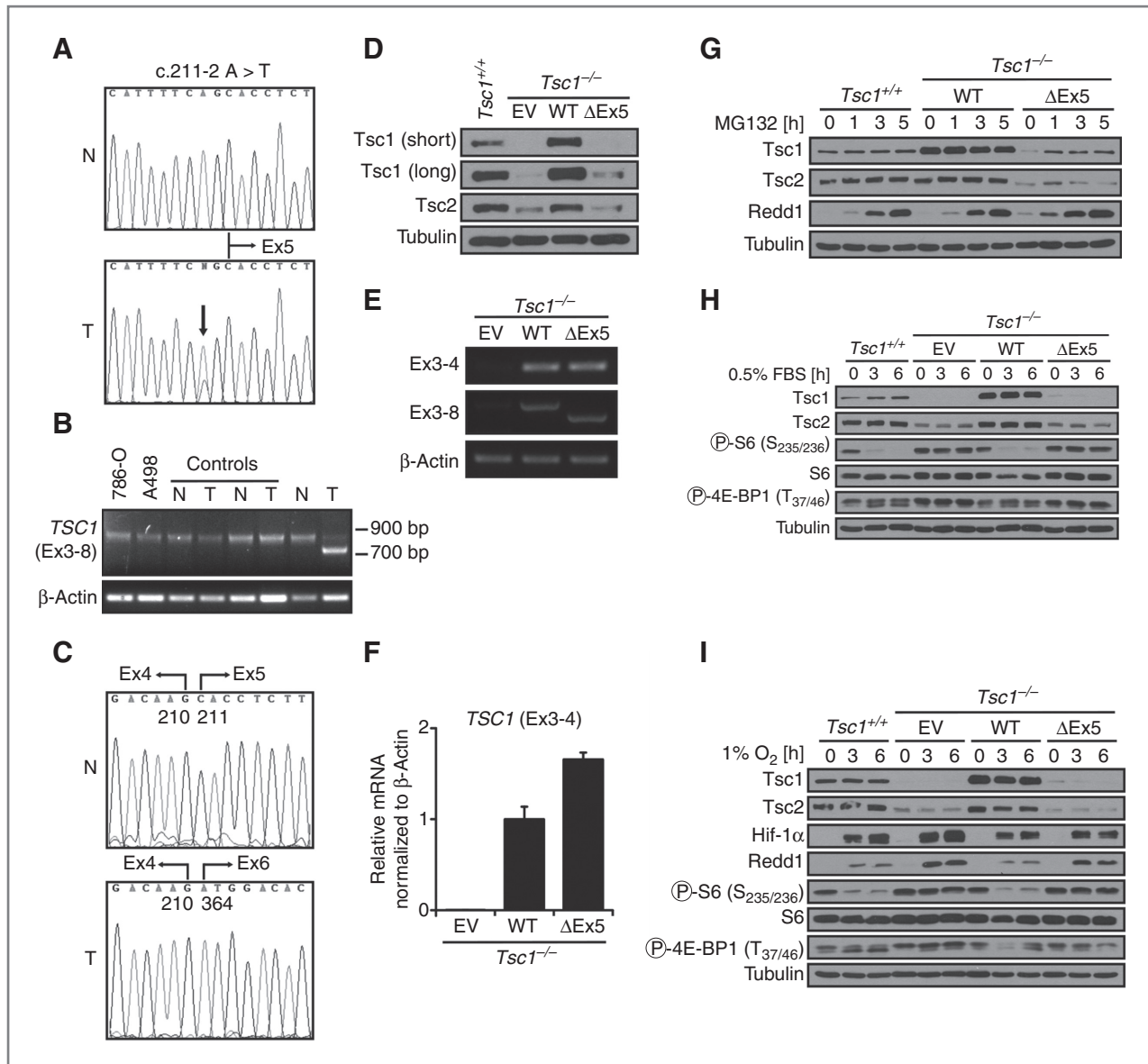


**Figure 5.** Characterization of a somatic *TSC1* mutation from a ccRCC tumor. A, sequence chromatograms of exon 5 splice acceptor in normal (N) and tumor (T; arrow indicates mutation). B, RT-PCR using primers in the indicated exons of normal (N) and tumor (T) samples compared with those from other patients and to ccRCC cell lines. C, cDNA sequence chromatograms of normal (N) and tumor (T) samples. D, immunoblot of immortalized *Tsc1*<sup>-/-</sup> MEFs (compared with immortalized *Tsc1*<sup>+/+</sup> MEFs) reconstituted with empty vector (EV), WT human *TSC1* or human *TSC1* deficient for exon 5 ( $\Delta$ Ex5). RT-PCR (E) and qRT-PCR (F) using primers in the indicated exons of *Tsc1*<sup>-/-</sup> MEFs reconstituted as indicated (data are means  $\pm$  SEM;  $n = 2$ ). G-I, immunoblot of MEFs of the indicated genotypes exposed to MG132 (G), serum withdrawal (H), and hypoxia (I) for the indicated number of hours.

*TSC1* were identified (Table 1). Matched normal samples were available for 2 tumors, which permitted confirmation that the mutations were somatically acquired. These mutations were both predicted to be truncating, and because truncating *TSC1* mutations further downstream have been associated with TSC syndrome (42), they are most likely pathogenic.

We sought to compare the mutation frequency of *TSC1* with that of *PTEN*, which has been previously implicated in

ccRCC (39, 40). As shown, in Table 1, *PTEN* sequencing of the same tumor cohort revealed a single *PTEN* mutation (p.G165V). This substitution was previously reported in association with Cowden syndrome (43) and is therefore pathogenic. Thus, *TSC1* mutations in ccRCC seem to occur at a frequency similar to, if not greater than, those in *PTEN*.

Because the *TSC1/TSC2* complex may also be inactivated by mutations in *TSC2*, *TSC2* coding and splice site sequences were similarly sequenced in the tumor cohort.

**Table 1.** Somatic mutations in ccRCC tumors

ID	Gene	cDNA	Protein
78	<i>REDD1</i>	c.550delC	Fs
9	<i>TSC1</i>	c.2459dupA	Fs
3246	<i>TSC1</i>	c.1546C > T	p.Q516X
4562	<i>TSC1</i>	IVS211-2A > T <sup>a</sup>	Sp
5533	<i>TSC1</i>	c.1342C > T <sup>b</sup>	p.P448S
4363	<i>PTEN</i>	c.494G > T	p.G165V

NOTE: Mutations within noncoding areas are prefixed with "IVS" and their position is identified by the number of nucleotides away from the closest coding sequence. Abbreviations: Fs, frame shift mutation; Sp, splice site mutation; ID, tumor identifier.

<sup>a</sup>Mutation in index patient's tumor.

<sup>b</sup>No normal tissue available.

However, no somatically acquired mutations were found in *TSC2*. Failure to identify *TSC2* mutations was not because of suboptimal sequencing as, equivalent to *TSC1* and *PTEN*, 100% of the *TSC2* amplicons were successfully sequenced across every one of the tumor samples.

Finally, we examined *REDD1*. As for *PTEN*, a single mutation was found in *REDD1* (Table 1). This mutation was predicted to be truncating and, because the C-terminus of *REDD1* is essential for its function (9), the mutation would be predicted to be inactivating.

Although no correlation was found between mutations and mTORC1 activation in tumors (Supplementary Table S1), only a few tumors had mutations, and we hypothesize that other mechanisms, genetic or epigenetic, account for mTORC1 activation despite *REDD1* induction in many other samples. Conspicuously, there were no concurrent mutations in *TSC1*, *REDD1*, and *PTEN*, a fact that could be explained simply by the low individual gene mutation frequency, but which may also indicate that the simultaneous occurrence of these mutations does not confer an additive advantage in ccRCC development and is therefore not selected for.

## Discussion

Herein, we evaluated the interplay between pVHL and mTORC1 pathways in ccRCC. We show that *REDD1* is upregulated in *VHL*-deficient ccRCC tumors, that *VHL* disruption is sufficient to upregulate *REDD1*, and that *REDD1* upregulation in ccRCC depends on pVHL and can be mediated by either HIF-1 or HIF-2. Furthermore, our data show that whereas *REDD1* is involved in restraining mTORC1 activity in some ccRCCs, in others, mechanisms have evolved to uncouple mTORC1 from *REDD1* inhibition. One such mechanism involves the disruption of the *TSC1/TSC2* complex and our results implicate *TSC1* as a novel tumor suppressor gene in sporadic ccRCC.

*REDD1* is broadly upregulated in *VHL*-deficient ccRCCs and *in vivo* as well as *in vitro* experiments indicate that *REDD1* regulation is *VHL* dependent. As *VHL* inactivation and HIF stabilization are thought to be among the earliest molecular events in renal tumorigenesis, it is not surprising that *REDD1* can already be observed upregulated in renal cysts in *VHL* patients (data not shown). *REDD1* upregulation in ccRCC requires HIF, and despite that differences exist in ccRCC depending upon whether HIF-1 $\alpha$  or HIF-2 $\alpha$  is expressed (24), both HIF-1 and HIF-2 are involved in the regulation of *REDD1*, and as supported by our CHIP studies, *REDD1* is directly acted upon by both. Nonetheless, should preferential regulation by HIF-1 occur in tumors, these data could contribute to explain why HIF-1 may function as a tumor suppressor in ccRCC.

Importantly, our results show that mTORC1 is regulated by *REDD1* in ccRCC in a context-dependent manner. The two extremes are illustrated by Caki-2 and 786-O cell lines. In Caki-2 cells, *REDD1* is engaged in mTORC1 inhibition suggesting that *REDD1* functions in a negative feedback loop to downregulate mTORC1 following *VHL* disruption. These data are consistent with the findings that acute disruption of *Vhl* in immortalized and primary MEFs has previously been shown to lead to senescence (44, 45). We conjecture that mTORC1 remains responsive to *REDD1* in Caki-2 cells because, as a consequence of a partially active pVHL, the level of *REDD1* upregulation is modest, such that the selective pressure to uncouple mTORC1 from *REDD1* is lower than in 786-O cells. By contrast, *REDD1* levels are high in 786-O cells, but mTORC1 is insensitive to it.

Loss of function mutations in *TSC1* activate mTORC1 and result in its uncoupling from *REDD1* as shown here with the *TSC1* splice site mutant. Three additional *TSC1* mutations were identified in the 77 tumors, including 2 truncating mutations that were confirmed to be somatically acquired. To our knowledge, this is the first report implicating *TSC1* as a tumor suppressor in sporadic ccRCC. As for *PTEN*, one somatically acquired inactivating mutation was found in *REDD1*, suggesting that, although rarely, mutations in *REDD1* may similarly contribute to ccRCC development.

In contrast to *TSC1*, somatic mutations in *TSC2* were not identified. A potential explanation for these findings would be furnished by the existence of a second tumor suppressor gene in the proximity of *TSC1* such that regional deletions may result in the simultaneous loss of the remaining wild-type copy for the 2 (or more) tumor suppressor genes. In fact, precedent for this exists in ccRCC and a tumor suppressor gene, *PBRM1*, was recently identified in relative proximity to *VHL* (46).

mTORC1 has been previously reported to be activated in 60% to 85% of ccRCCs (1, 2). Although these studies were based on phospho-S6<sup>S235/236</sup> signal, which is thought to be less specific than phospho-S6<sup>S240/244</sup> (37), we found that approximately 80% of ccRCC were positive for phospho-S6<sup>S240/244</sup>, adding support to the notion that mTORC1 is broadly activated in this tumor type.

Given the low frequency of mutations in *TSC1* and *PTEN*, other mechanisms must exist to prevent mTORC1 inhibition by REDD1. Although targeted sequencing studies have failed to identify activating mutations in *Rheb* and *RhebL1* (2), recently, mutations in the *mTOR* gene itself were identified in ccRCC (32, 46). Furthermore, tumor-associated *mTOR* mutants have been found to lead to mTORC1 activation and diminished mTORC1 inhibition by hypoxia (47). Nevertheless, these mutations are also rare. It is also possible that inactivation of a single *TSC1* allele, and *TSC1* is found in 9q, a region that is deleted in approximately 20% of ccRCC (31, 48), may be sufficient to activate mTORC1 and render it unresponsive to REDD1. In keeping with this idea, modest depletion of *TSC2* appears to be sufficient to block REDD1-induced mTORC1 inhibition (8).

Understanding how mTORC1 is deregulated in ccRCC may pave the way for the identification of patients most likely to benefit from mTORC1 inhibitors. It would be expected that only tumors with active mTORC1 respond to its inhibition and this is supported by a small retrospective correlative study (49). Although the phosphorylation state of mTORC1 effector proteins may be used as the readout for mTORC1 activation, TORC1 is a critical regulator of ribosomal biogenesis and nucleolar size (50, 51) and conceivably, nucleolar dimensions could serve as a surrogate for mTORC1 activity in tumors. In RCC, nucleolar prominence is a major determinant of the prognostic Fuhrman grading scale (52). The regulation of nucleolar size by mTORC1 provides an explanation for the positive correlation previously reported between phospho-S6 and tumor grade (1). This raises the possibility that the activation state of mTORC1 may contribute to the prognostic significance of the Fuhrman grading scale. Furthermore, it is possible that nucleolar size could serve as a pharmacodynamic indicator of mTORC1 inhibition in RCC. Should nucleolar prominence be dynamically regulated by mTORC1, the exposure of patients to mTORC1 inhibitors could affect Fuhrman grading. Supporting this concern, rapamycin was previously shown to reduce nucleolar size in both mammalian and yeast cells (51).

Driver mutations in tumors may reflect a state of addiction that could be exploited therapeutically. In this context,

and despite that the TSC1/TSC2 complex likely regulates other processes besides mTORC1 (53, 54), mutations in *TSC1* in ccRCC could portend a state of addiction to mTORC1. Although this represents a single instance, it is noteworthy that the index patient who had the original *TSC1* splice site mutation we evaluated had an extraordinary response to everolimus in the second line. Although the median progression-free interval on everolimus in the second line in the pivotal phase III clinical trial was 4 months (4), the patient remained on everolimus without progression for 13 months, and this was despite progression to sunitinib in 3 months.

In summary, this work begins to unravel the complexity of signaling pathways linking pVHL and mTORC1 in ccRCC and suggests that mechanisms have evolved in tumors to escape growth suppressive signals resulting from *VHL* loss and REDD1 upregulation.

### Disclosure of Potential Conflicts of Interest

REDD1 monoclonal antibody reported herein is licensed to Bethyl laboratories.

### Acknowledgments

We thank Dr. William G. Kaelin, Jr. for the gift of pRC3, WT8 cell lines, and the *VHL* expression vector; Linda Donnelly and Y. K. Ho (Molecular Genetics, UTSW Medical Center) for generation of hybridomas used for REDD1 monoclonal antibody production, Ping Shang for help with REDD1 immunohistochemistry, and members of the Brugarolas lab for helpful discussions.

### Grant Support

This work was supported by NIH (R01CA129387, K08NS051843, T32CA124334, F32CA126087), March of Dimes, Doris Duke, V Foundation, and Generalitat Valenciana. S. Peña-Llopis was supported in part by a fellowship of Excellence from the Generalitat Valenciana (BPOSTDOC06/004) and T.A.T. Tran by F32CA126087 and T32CA124334. J. Brugarolas was supported by the following grants: K08NS051843 and R01CA129387, a Basil O'Connor Starter Scholar Research Award (5FY06582), a Doris Duke Clinical Scientist Development Award (2007062), and a V Scholar Award. J. Brugarolas is a Virginia Murchison Linthicum Scholar in Medical Research at UT Southwestern.

The costs of publication of this article were defrayed in part by the payment of page charges. This article must therefore be hereby marked *advertisement* in accordance with 18 U.S.C. Section 1734 solely to indicate this fact.

Received June 27, 2011; accepted July 18, 2011; published OnlineFirst July 28, 2011.

### References

- Pantuck AJ, Seligson DB, Klatt T, Yu H, Leppert JT, Moore L, et al. Prognostic relevance of the mTOR pathway in renal cell carcinoma: implications for molecular patient selection for targeted therapy. *Cancer* 2007;109:2257-67.
- Robb VA, Karbowniczek M, Klein-Szanto AJ, Henske EP. Activation of the mTOR signaling pathway in renal clear cell carcinoma. *J Urol* 2007;177:346-52.
- Hudes G, Carducci M, Tomczak P, Dutcher J, Figlin R, Kapoor A, et al. Temsirolimus, interferon alfa, or both for advanced renal-cell carcinoma. *N Engl J Med* 2007;356:2271-81.
- Motzer RJ, Escudier B, Oudard S, Hutson TE, Porta C, Bracarda S, et al. Efficacy of everolimus in advanced renal cell carcinoma: a double-blind, randomised, placebo-controlled phase III trial. *Lancet* 2008;372:449-56.
- Wullschlegler S, Loewith R, Hall MN. TOR signaling in growth and metabolism. *Cell* 2006;124:471-84.
- Zoncu R, Efeyan A, Sabatini DM. mTOR: from growth signal integration to cancer, diabetes and ageing. *Nat Rev Mol Cell Biol* 2011;12:21-35.
- Gingras AC, Raught B, Sonenberg N. Regulation of translation initiation by FRAP/mTOR. *Genes Dev* 2001;15:807-26.
- Brugarolas J, Lei K, Hurley RL, Manning BD, Reiling JH, Hafen E, et al. Regulation of mTOR function in response to hypoxia by REDD1 and the TSC1/TSC2 tumor suppressor complex. *Genes Dev* 2004;18:2893-904.
- Vega-Rubin-de-Celis S, Abdallah Z, Kinch L, Grishin NV, Brugarolas J, Zhang X. Structural analysis and functional implications of the negative mTORC1 regulator REDD1. *Biochemistry* 2010;49:2491-501.

10. Shoshani T, Faerman A, Mett I, Zelin E, Tenne T, Gorodin S, et al. Identification of a novel hypoxia-inducible factor 1-responsive gene, RTP801, involved in apoptosis. *Mol Cell Biol* 2002;22:2283–93.
11. Schwarzer R, Tondera D, Arnold W, Giese K, Klippel A, Kaufmann J. REDD1 integrates hypoxia-mediated survival signaling downstream of phosphatidylinositol 3-kinase. *Oncogene* 2005;24:1138–49.
12. Jin HO, An S, Lee HC, Woo SH, Seo SK, Choe TB, et al. Hypoxic condition- and high cell density-induced expression of Redd1 is regulated by activation of hypoxia-inducible factor-1alpha and Sp1 through the phosphatidylinositol 3-kinase/Akt signaling pathway. *Cell Signal* 2007;19:1393–403.
13. Otulakowski G, Duan W, Sarangapani A, Gandhi S, O'Brodovich H. Glucocorticoid-mediated repression of REDD1 mRNA expression in rat fetal distal lung epithelial cells. *Pediatr Res* 2009;65:514–9.
14. Regazzetti C, Bost F, Le Marchand-Brustel Y, Tanti JF, Giorgetti-Peraldi S. Insulin induces REDD1 expression through hypoxia-inducible factor 1 activation in adipocytes. *J Biol Chem* 2010;285:5157–64.
15. Avruch J, Long X, Ortiz-Vega S, Rapley J, Papageorgiou A, Dai N. Amino acid regulation of TOR complex 1. *Am J Physiol Endocrinol Metab* 2009;296:E592–602.
16. Corradetti MN, Inoki K, Guan KL. The stress-induced proteins RTP801 and RTP801L are negative regulators of the mammalian target of rapamycin pathway. *J Biol Chem* 2005;280:9769–72.
17. Sofer A, Lei K, Johannessen CM, Ellisen LW. Regulation of mTOR and cell growth in response to energy stress by REDD1. *Mol Cell Biol* 2005;25:5834–45.
18. Cai SL, Tee AR, Short JD, Bergeron JM, Kim J, Shen J, et al. Activity of TSC2 is inhibited by AKT-mediated phosphorylation and membrane partitioning. *J Cell Biol* 2006;173:279–89.
19. DeYoung MP, Horak P, Sofer A, Sgroi D, Ellisen LW. Hypoxia regulates TSC1/2-mTOR signaling and tumor suppression through REDD1-mediated 14-3-3 shuttling. *Genes Dev* 2008;22:239–51.
20. Crino PB, Nathanson KL, Henske EP. The tuberous sclerosis complex. *N Engl J Med* 2006;355:1345–56.
21. Parry L, Maynard JH, Patel A, Clifford SC, Morrissey C, Maher ER, et al. Analysis of the TSC1 and TSC2 genes in sporadic renal cell carcinomas. *Br J Cancer* 2001;85:1226–30.
22. Nickerson ML, Jaeger E, Shi Y, Durocher JA, Mahurkar S, Zaridze D, et al. Improved identification of von Hippel-Lindau gene alterations in clear cell renal tumors. *Clin Cancer Res* 2008;14:4726–34.
23. Kaelin WG Jr., Ratcliffe PJ. Oxygen sensing by metazoans: the central role of the HIF hydroxylase pathway. *Mol Cell* 2008;30:393–402.
24. Gordan JD, Lal P, Dondeti VR, Letrero R, Parekh KN, Oquendo CE, et al. HIF-1alpha effects on c-Myc distinguish two subtypes of sporadic VHL-deficient clear cell renal carcinoma. *Cancer Cell* 2008;14:435–46.
25. Kucejova B, Sunny NE, Nguyen AD, Hallac R, Fu X, Peña-Llopis S, et al. Uncoupling hypoxia signaling from oxygen sensing in the liver results in hypoketotic hypoglycemic death. *Oncogene* 2011.
26. Whaley JM, Naglich J, Gelbert L, Hsia YE, Lamiell JM, Green JS, et al. Germ-line mutations in the von Hippel-Lindau tumor-suppressor gene are similar to somatic von Hippel-Lindau aberrations in sporadic renal cell carcinoma. *Am J Hum Genet* 1994;55:1092–102.
27. van Houwelingen KP, van Dijk BA, Hulsbergen-van de Kaa CA, Schouten LJ, Gorissen HJ, Schalken JA, et al. Prevalence of von Hippel-Lindau gene mutations in sporadic renal cell carcinoma: results from The Netherlands cohort study. *BMC Cancer* 2005;5:57.
28. Iliopoulos O, Kibel A, Gray S, Kaelin WG Jr. Tumour suppression by the human von Hippel-Lindau gene product. *Nat Med* 1995;1:822–6.
29. Mole DR, Blancher C, Copley RR, Pollard PJ, Gleadle JM, Ragoussis J, et al. Genome-wide association of hypoxia-inducible factor (HIF)-1alpha and HIF-2alpha DNA binding with expression profiling of hypoxia-inducible transcripts. *J Biol Chem* 2009;284:16767–75.
30. Hu CJ, Wang LY, Chodosh LA, Keith B, Simon MC. Differential roles of hypoxia-inducible factor 1alpha (HIF-1alpha) and HIF-2alpha in hypoxic gene regulation. *Mol Cell Biol* 2003;23:9361–74.
31. Beroukhim R, Brunet JP, Di Napoli A, Mertz KD, Seeley A, Pires MM, et al. Patterns of gene expression and copy-number alterations in von Hippel-Lindau disease-associated and sporadic clear cell carcinoma of the kidney. *Cancer Res* 2009;69:4674–81.
32. Daigliesh GL, Furge K, Greenman C, Chen L, Bignell G, Butler A, et al. Systematic sequencing of renal carcinoma reveals inactivation of histone modifying genes. *Nature* 2010;463:360–3.
33. Hu CJ, Iyer S, Sataur A, Covello KL, Chodosh LA, Simon MC. Differential regulation of the transcriptional activities of hypoxia-inducible factor 1 alpha (HIF-1alpha) and HIF-2alpha in stem cells. *Mol Cell Biol* 2006;26:3514–26.
34. Denko NC, Fontana LA, Hudson KM, Sutphin PD, Raychaudhuri S, Altman R, et al. Investigating hypoxic tumor physiology through gene expression patterns. *Oncogene* 2003;22:5907–14.
35. Wang V, Davis DA, Haque M, Huang LE, Yarchoan R. Differential gene up-regulation by hypoxia-inducible factor-1alpha and hypoxia-inducible factor-2alpha in HEK293T cells. *Cancer Res* 2005;65:3299–306.
36. Wolff NC, Vega-Rubin-de-Celis S, Xie XJ, Castrillon DH, Kabbani W, Brugarolas J. Cell type-dependent regulation of mTORC1 by REDD1 and the tumor suppressors TSC1/TSC2 and LKB1 in response to hypoxia. *Mol Cell Biol* 2011.
37. Anjum R, Blenis J. The RSK family of kinases: emerging roles in cellular signalling. *Nat Rev Mol Cell Biol* 2008;9:747–58.
38. Available from: [www.sanger.ac.uk/genetics/CGP/CellLines](http://www.sanger.ac.uk/genetics/CGP/CellLines).
39. Alimov A, Li C, Gizatullin R, Fredriksson V, Sundelin B, Klein G, et al. Somatic mutation and homozygous deletion of PTEN/MMAC1 gene of 10q23 in renal cell carcinoma. *Anticancer Res* 1999;19:3841–6.
40. Kondo K, Yao M, Kobayashi K, Ota S, Yoshida M, Kaneko S, et al. PTEN/MMAC1/TEP1 mutations in human primary renal-cell carcinomas and renal carcinoma cell lines. *Int J Cancer* 2001;91:219–24.
41. Available from: [www.sanger.ac.uk/genetics/CGP/cosmic/](http://www.sanger.ac.uk/genetics/CGP/cosmic/).
42. Available from: [http://chromium.liacs.nl/LOVD2/TSC/home.php?select\\_db=TSC1](http://chromium.liacs.nl/LOVD2/TSC/home.php?select_db=TSC1).
43. Available from: [www.uniprot.org/uniprot/P60484](http://www.uniprot.org/uniprot/P60484).
44. Mack FA, Patel JH, Biju MP, Haase VH, Simon MC. Decreased growth of Vhl-/- fibrosarcomas is associated with elevated levels of cyclin kinase inhibitors p21 and p27. *Mol Cell Biol* 2005;25:4565–78.
45. Young AP, Schlisio S, Minamishima YA, Zhang Q, Li L, Grisanzio C, et al. VHL loss actuates a HIF-independent senescence programme mediated by Rb and p400. *Nat Cell Biol* 2008;10:361–9.
46. Varela I, Tarpey P, Raine K, Huang D, Ong CK, Stephens P, et al. Exome sequencing identifies frequent mutation of the SWI/SNF complex gene PBRM1 in renal carcinoma. *Nature* 2011;469:539–42.
47. Sato T, Nakashima A, Guo L, Coffman K, Tamanoi F. Single amino acid changes that confer constitutive activation of mTOR are discovered in human cancer. *Oncogene* 2010;29:2746–52.
48. Chen M, Ye Y, Yang H, Tamboli P, Matin S, Tannir NM, et al. Genome-wide profiling of chromosomal alterations in renal cell carcinoma using high-density single nucleotide polymorphism arrays. *Int J Cancer* 2009;125:2342–8.
49. Cho D, Signoretti S, Dabora S, Regan M, Seeley A, Mariotti M, et al. Potential histologic and molecular predictors of response to temsirinolimus in patients with advanced renal cell carcinoma. *Clin Genitourin Cancer* 2007;5:379–85.
50. Zhang H, Stallock JP, Ng JC, Reinhard C, Neufeld TP. Regulation of cellular growth by the Drosophila target of rapamycin dTOR. *Genes Dev* 2000;14:2712–24.
51. Tsang CK, Bertram PG, Ai W, Drenan R, Zheng XF. Chromatin-mediated regulation of nucleolar structure and RNA Pol I localization by TOR. *EMBO J* 2003;22:6045–56.
52. Fuhrman SA, Lasky LC, Limas C. Prognostic significance of morphologic parameters in renal cell carcinoma. *Am J Surg Pathol* 1982;6:655–63.
53. Brugarolas JB, Vazquez F, Reddy A, Sellers WR, Kaelin WG Jr. TSC2 regulates VEGF through mTOR-dependent and -independent pathways. *Cancer Cell* 2003;4:147–58.
54. Peña-Llopis S, Vega-Rubin-de-Celis S, Schwartz JC, Wolff NC, Tran TA, Zou L, et al. Regulation of TFEB and V-ATPases by mTORC1. *EMBO J* 2011;30:3242–58.